10.1098/rsta.2000.0814

THE ROYAL SOCIETY

Development of model colloidal liquid crystals and the kinetics of the isotropic–smectic transition

By Zvonimir Dogic and Seth Fraden

The Complex Fluid Group, Martin Fisher School of Physics, Brandeis University, Waltham, MA 02454, USA

We have prepared a homologous series of filamentous viruses with varying contour length using molecular cloning techniques. These viruses are monodisperse enough to form a stable smectic phase. Two systems are studied. The first system consists of viruses to the surfaces of which the polymers are covalently bound. Through studies of the isotropic–cholesteric phase transition we demonstrate that covalently attached polymers alter the effective diameter of the virus. Additionally, we have produced mixtures of viruses whose ratio of effective diameters varies by a factor of five. The second system is composed of mixtures of rod-like viruses and non-absorbing Gaussian polymers. With this system we study the kinetics of the isotropic–smectic phase transition and describe observations of a number of novel metastable structures of unexpected complexity.

Keywords: depletion interaction; hard-rod fluids; virus; filamentous phage

1. Introduction

Observation of the nematic phase in aqueous suspensions of rod-like tobacco mosaic virus (TMV) served as an inspiration for Onsager to write his seminal paper on the isotropic–nematic (I–N) phase transition in hard rods (Onsager 1949). Ever since then, biopolymers (DNA, TMV, fd) have served as an important model system of hard rods and have often been used to test the Onsager theory and its various extensions (Meyer 1990; Fraden 1995; Livolant 1991). In § 2 of this paper we briefly outline the advantages of using the semi-flexible rod-like fd or closely related M13 virus as a model system of hard rods. We demonstrate that, using standard procedures of molecular cloning, it is possible to construct genetically modified viruses with widely varying contour length. These viruses are monodisperse enough to form a stable smectic phase. In § 3 we outline the synthesis of an fd-polymer complex and show that polymers covalently attached to the virus effectively increase the diameter of the rods. By changing the ionic strength, it is possible to observe the crossover from the regime where the rods are electrostatically stabilized to that where they are sterically stabilized by repulsion between virus-bound polymers. This synthesis is a convenient way to alter the diameter of the rod and enables us to study bidisperse rod suspensions with different diameters. In § 4 we outline the phase behaviour of mixtures of fd virus with non-absorbing polymer. In particular, we focus on the isotropic–smectic phase transition and describe a number of different pathways by which the smectic phase nucleates and grows out of an isotropic suspension of viruses.

2. fd virus as a versatile model system of hard rods

TMV and fd viruses form, in order of increasing concentration of rods, a stable isotropic, nematic or cholesteric, and smectic phase (Wen *et al.* 1989; Dogic & Fraden 1997, 2000). These two experimental colloidal systems are the only ones that follow the sequence of liquid crystalline phase transitions that have been predicted by the theory and computer simulations of hard rods (Bolhuis & Frenkel 1997; Vroege & Lekkerkerker 1992). The paucity of systems exhibiting smectic phases is presumably due to polydispersity, which is inherently present in all other polymeric and colloidal experimental systems due to the fact that they are chemically synthesized. In contrast to chemical synthesis, nature uses DNA technology to produce viruses that are identical to each other, which results in highly monodisperse viruses. This high monodispersity of virus suspensions is the property that makes them an appealing system to study the phase behaviour of hard rods experimentally.

However, there are several important disadvantages that viruses have, compared with synthetic rod-like polymers. Firstly, although rod-like viruses have very well-defined lengths and diameters, studies of how the phase behaviour depends on the length-to-diameter ratio are non-existent for virus suspensions. Secondly, the viruses are charge stabilized, and therefore their interactions are not truly hard-rod interactions, but, in addition to steric repulsion, have a long-range soft repulsion. It is important to note that because of the small diameter of the virus, the range of this electrostatic repulsion is always comparable to the hard core diameter for the range of ionic strengths for which the stability of the virus against aggregation is not compromised. Also, because of its protein structure, it is impossible to decrease the surface charge by dissolving it in apolar or weakly polar solvents and to preserve the colloidal stability of the virus. It has also been observed that the virus aggregates in an ionic solution of multivalent cations. In this section we show that, using standard biological methods, it is possible to alter the contour length of the virus while preserving the monodispersity of the virus. In the subsequent section we show that by covalently attaching polymers onto the virus surface we can alter the effective diameter of the virus, and we have achieved stability of the virus even in the presence of multivalent cations. It is our hope that the introduction of these methods will make the viruses a more appealing model system with which to study the phase behaviour of rods.

We note that the M13 virus with length (L) diameter (D) ($L/D \approx 130$) and construct M13-T_n3-15 ($L/D \approx 240$) was used in the studies of the concentration dependence of rotational diffusion almost 20 years ago (Maguire *et al.* 1980). However, this potentially powerful method was never pursued in subsequent studies. M13 virus is genetically almost identical to fd and has the same contour length, with coat proteins differing by only a single amino acid; negatively charged aspartate in fd (asp_{12}) corresponding to neutral asparagine in M13 (asn_{12}) (Bhattacharjee *et al.* 1992). This change in a single amino acid alters the surface charge by *ca.* 30% and M13 can easily be distinguished from fd by gel electrophoresis. All our clones have their origin in M13 virus, which also means that they have a lower surface charge than fd wild-type system.

Since all available data indicate that the length of the virus is linearly proportional to the length of the DNA contained in the virus, the virus length can be extended by simply introducing foreign DNA into M13 wild-type DNA using restriction endonu-

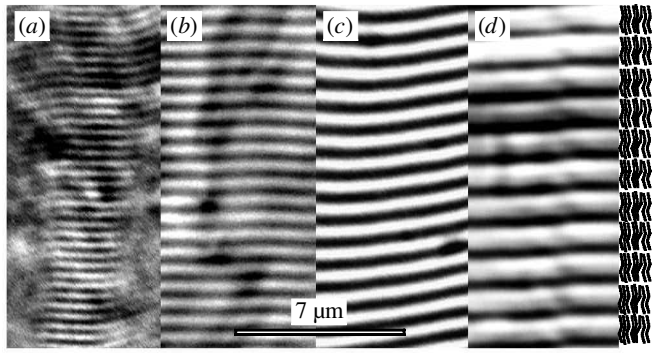

Figure 1. Optical differential interference contrast (DIC) micrographs of smectic phases of three different M13 constructs and fd wild type (*c*). The periodic pattern is due to smectic layers that are composed of two-dimensional liquids of essentially parallel rods, as indicated in the cartoon on the right. From left to right, the contour lengths of the rod-like viruses forming the smectic phase are 0.39, 0.64, 0.88 and 1.2 μm. The smectic spacings measured from optical micrographs are 0.40, 0.64, 0.9 and 1.22 μm from image (*a*) to (*d*), respectively.

cleases (Herrmann *et al*. 1980). However, during large-scale preparation we found that the mutant virus would often quickly revert to its wild-type form by deleting the foreign DNA. Another disadvantage of this method is that it is impossible to construct clones that are shorter than M13 wild type. Because of these reasons, we used a well-documented phagemid method to prepare our rod-like viruses with variable contour length (Maniatis *et al*. 1989). This method allows us to grow clones that are both longer and shorter then M13 wild type. The disadvantage of the phagemid method is that the helper phage M13KO7 (a virus with contour length 1.2 μm) is always present in the final suspension. The volume fraction of the helper phage depends on the bacterial host and can vary from 20% (*E. coli* JM 101) to 5% (*E. coli* XL-1 Blue). Typically, 0.5–1 g of purified virus can be obtained in one to two weeks of work. We found that it is possible to separate the clones from the 1.2 μm long helper phage by adjusting the concentration of the bidisperse purified virus suspension such that it is in I–N coexistence. There is a strong fractionation effect at the I–N transition for bidisperse rods, with large rods almost entirely dispersed in nematic phase, as is predicted by the theory (Lekkerkerker *et al*. 1984; Sato & Teramoto 1994). Therefore, by keeping only the portion of the suspension in the isotropic phase, we can obtain rods with higher monodispersity.

All of the viruses grown using the phagemid method are monodisperse enough to form stable smectic phases, as is illustrated in figure 1. We note that the measured spacing of the smectic phase (λ) is almost identical to the contour length (L) for all the mutants studied. The qualitative trend that flexibility decreases the smectic layering has been predicted theoretically and observed experimentally (Dogic & Fraden 1997; Polson & Frenkel 1997; van der Schoot 1996; Tkachenko 1996). Unfortunately, the theories are not accurate enough to be able to quantitatively predict the dependence of smectic spacing on the flexibility of the rod. We expect that the persistence length ($P \sim 2.2\,\mu$m) of all our clones is the same, because all clones have the same structure and only vary in length. Since the contour length varies, so too does the ratio of contour to persistence length L/P. Thus we expected that the shorter rods ($L = 0.4\,\mu$m) would be relatively stiffer than the longer ones ($L = 1.4\,\mu$m) and con-

sequently predicted that the layer spacing would increase for shorter rods. This was not the case, as we observed that for all lengths the ratio $\lambda/L \sim 1$.

We also discovered that fd wild type (figure 1*c*) consistently forms a smectic phase at a lower concentration than M13 constructs. This is perhaps explained by the difference in surface charge between M13 and fd and the breakdown of the concept of effective diameter at high concentrations. The fd wild type is more charged than M13 and therefore the highly concentrated aligned rods in the nematic phase repel each other more strongly, which results in a higher effective concentration and thus the nematic–smectic phase transition occurs at a lower number density of rods. Note that, at low concentrations, changing the surface charge by 30% has negligible effect on the effective diameter and the phase behaviour of the isotropic–nematic transition (Tang & Fraden 1995, fig. 1).

With the availability of rods with different contour length we are able to experimentally explore a number of important issues pertaining to the phase behaviour of hard rods. For pure rods, we can address the question of how flexible a particle can be and still form a smectic phase. Another important question is the relative stability of the columnar and smectic phase as a function of rod bidispersity or polydispersity (Bates & Frenkel 1998; Bohle *et al*. 1996; Stroobants 1992; van Roij & Mulder 1996; Cui & Chen 1994). For mixtures whose lengths are different enough, there is also a prediction of microseparated smectic phase (Koda & Kimura 1994). So far, there are no experimental studies on these subjects, but with our system we can prepare artificially polydisperse and bidisperse suspensions to explore these issues.

3. fd virus with covalently attached polymer

Besides preparing viruses with varying contour length, we are also able to alter the effective diameter of the virus by coating it with polymer. The amino terminal group of each coat protein of fd and M13 virus is exposed to the solution. Through this chemical site we are able to covalently attach water soluble polymer poly(ethylene glycol) (PEG) to the surface of the virus. End functionalized PEG molecules that readily attach to amino groups were obtained from Shearwater polymers. The chemical reaction was carried out in 100 mM phophate buffer at pH 7.5 for 30 min and the virus concentration was kept at 1 mg ml^{-1}. For SSA–PEG-5000, the weight concentration of PEG was kept the same as the weight concentration of the virus in the reaction vessel, while for SPA–PEG-20 000, the concentration was four times the virus concentration. The reaction product (fd–PEG) was separated from unreacted PEG polymer by repeated centrifugation at 200 000*g*. The pellet contained the nematic phase of the fd–PEG complex. We diluted a few samples to the concentration of the isotropic–nematic phase coexistence, and after an exceedingly long time (up to a few months), we observed macroscopic phase separation. The measured width of the coexisting concentrations did not differ from the measured width in fd wild type, which is *ca.* 10% (Tang & Fraden 1995). This is an indication that the absorbed polymer does not significantly alter the flexibility of the rod-like particles. We infer this from the well-established fact that the width of the I–N coexistence is very sensitive to the flexibility of the rod (Chen 1993). If we had observed widening of the I–N coexistence, it would have been an indication that polymer effectively increases rigidity of the rod. Because of the extremely long time required for complete phase separation, in order to obtain the points in figure 2, we diluted the nematic phase

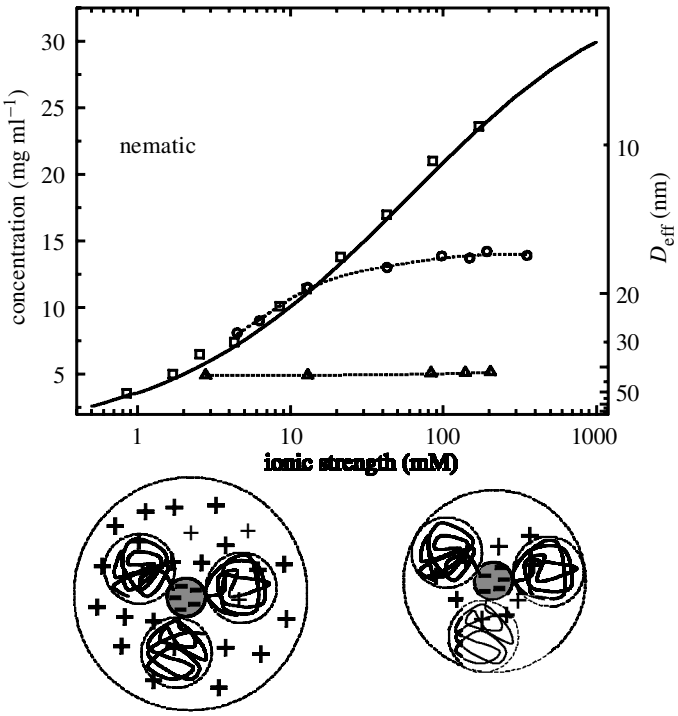

Figure 2. Concentration of the virus rods in coexisting isotropic and nematic phases as a function of ionic strength and thickness of a PEG layer covalently attached to the virus. Square points indicate the I–N transition in bare fd wild type and were taken from previous work (Tang & Fraden 1995). The relationship between the I–N coexistence concentration (c) and electrostatic effective diameter is c (mg ml^{-1}) $= 222/D_{\mathrm{eff}}$ (nm) and is drawn as a solid line. Circles indicate the I–N transition in fd coated with 5000 MW PEG, while triangles refer to the fd virus coated with 20 000 MW PEG. When calculating the concentration of fd–PEG, we only take into account the fd core, since the polymer density is not known. The dashed lines are a guide for the eye. At low ionic strength, electrostatic repulsion determines D_{eff}, while the grafted polymer sets D_{eff} at high ionic strength, as indicated in the cartoon of a cross-section of the negatively charged virus–PEGs complex.

until there was no more birefringence observed. We presume that this concentration is equal to the concentration of rods in isotropic phase coexisting with the nematic phase.

To interpret the data in figure 2, we need to introduce the concept of the effective diameter (D_{eff}). The isotropic–nematic phase transition for very long rods can be described at the level of the second virial coefficient, as was first recognized by Onsager (1949). The prediction of the theory is that the isotropic phase becomes unstable when the following condition is satisfied, $\frac{1}{4}c\pi L^2 D = 4$, where c is rod number density, while L and D are the length and the diameter of the rod. In the same paper, Onsager showed how to incorporate the effect of long-range repulsion due to surface charge by exchanging the bare diameter with an effective diameter D_{eff}, which can be rigorously calculated and is roughly equal to the distance between two rods where the intermolecular potential is equal to thermal energy of $1k_{\mathrm{B}}T$. At high ionic strength, D_{eff} approaches the bare diameter, while at low ionic strength,

D_{eff} is much larger than the bare diameter, and is typically several Debye screening lengths. The condition for the instability of the isotropic phase for charged rods becomes $\frac{1}{4}c\pi L^2 D_{\mathrm{eff}} = 4$. It follows that the bare rod number density at the I–N phase transition is inversely proportional to D_{eff}. This is experimentally observed for fd wild type over a wide range of ionic strengths, as shown with square symbols in figure 2. The full line, which contains no adjustable parameters, is the numerical solution of the I–N transition for semiflexible rods, where D_{eff} is calculated by an extension of the Onsager theory (Chen 1993). For clarification, we note that fd forms a cholesteric, not nematic, phase, but the free-energy difference between these two phases is negligible compared with the free-energy difference between the isotropic and nematic phases (Tang & Fraden 1995; Dogic & Fraden 2000).

Water at room temperature is a good solvent for PEG polymers, which approximate Gaussian coils. Thus PEG coated surfaces interact with each other through long-range repulsion (Devanand & Selser 1991; Kuhl *et al.* 1994). Therefore, in our fd–PEG system, in addition to the already present electrostatic repulsion between the charged virus surfaces, we introduce repulsion due to the attached PEG molecules. We expect that for polymers with large molecular weight and/or at high ionic strength, the dominant interparticle interaction, and consequently D_{eff}, is completely determined by the polymer diameter because the ionic double layer is confined deep within the attached polymer. The opposite is true at low ionic strength and/or low molecular weight polymer. This is exactly the behaviour that is shown in figure 2. For fd grafted with 20 k MW PEG (fd–PEG-20 000), we observe that for ionic strengths greater than 2 mM, the I–N transition is independent of ionic strength. This implies that D_{eff} for the fd–PEG-20 000 system is determined entirely by polymer repulsion. The effective diameter of the particle can be extracted from the I–N coexistence concentrations, since we have shown that there is a relationship between the effective diameter and concentration of virus, $c\ (\mathrm{mg\ ml^{-1}}) = 222/D_{\mathrm{eff}}\ (\mathrm{nm})$. For fd–PEG-5000, the I–N transition changes from being dominated by polymer stabilization at high ionic strength to electrostatic stabilization below 20 mM ionic strength. Because this transition from polymer dominated to electrostatic dominated repulsion occurs at a higher ionic strength for fd–PEG-5000 compared with fd–PEG-20 000, the effective diameter of fd–PEG-5000 is smaller than that for fd–PEG-20 000. The formula relating the molecular weight (M_{w}) of PEG to its radius of gyration (R_{g}) is $R_{\mathrm{g}} = 0.215 M_{\mathrm{w}}^{0.583}$ Å (Devanand & Selser 1991). From figure 2 we can calculate that the fd–PEG-20 000 system has $D_{\mathrm{eff}} = 45$ nm, which is approximately equal to $D_{\mathrm{bare}} + 4R_{\mathrm{g}} = 35$ nm. fd–PEG-5000 complex has $D_{\mathrm{eff}} = 17$ nm at high ionic strength, while $D_{\mathrm{bare}} + 4R_{\mathrm{g}} = 19$ nm. This suggests the model of the polymer being a sphere of radius R_{g} attached to the surface of the virus, although we expect that the polymer is deformed by the virus to some extent. In principle, if the exact shape of the repulsive interaction between two polymer-covered cylindrical surfaces is known, and if the number of attached polymers per virus is measured, it would be possible to theoretically calculate the phase diagram for rods with attached polymers and compare it with experimental findings. However, we have not yet developed a method to accurately measure the polymer surface coverage.

We can use our system of rods with different diameters to study some basic problems in the physics of colloidal liquid crystals. To prepare a binary mixture of rods with different diameters, we simply mix fd wild type and fd–PEG. The ratio of the diameters is equal to the ratio of the concentrations at which these two systems

undergo the I–N transition. An additional advantage of this system is that this ratio can be altered in a continuous way by simply adjusting ionic strength. From figure 2 it is possible to deduce that at 200 mM ionic strength the fd–PEG complex has an effective diameter about five times thicker than fd wild type. We have observed both isotropic–isotropic and nematic–nematic demixing in binary mixtures of fd–PEG-20 000 and fd wild type. Comparison to available theories is currently underway (van Roij & Mulder 1998; Sear & Mulder 1996). In summary, a combination of molecular engineering and post-expression chemistry has resulted in the production of gram quantities of monodisperse rods varying in length from 0.4–1.4 μm and diameter 10–50 nm.

4. Phase behaviour of fd wild-type virus with non-absorbing polymer

Onsager has shown how to describe the I–N transition of hard rods with large L/D ratio using the virial expansion of free-energy. The second virial expansion quantitatively describes very long and thin rods at the isotropic–nematic coexistence, but fails for highly aligned and concentrated rods. As explained in the previous section, even systems that have soft repulsion can be successfully described by the Onsager theory. The reason for this is that the lowest energy state occurs when two charged rods are perpendicular to each other. Therefore, charge reduces alignment of the rods, which in turn increases the accuracy of the virial expansion (Stroobants *et al.* 1986). In contrast, if there is attraction between rods, then perfectly parallel rods are the configuration with the lowest energy. Consequently, attractions increase the overall alignment of the rods in a nematic suspension and decrease the accuracy with which the virial expansion describes the system. It was shown that for even very slightly attractive rods the third virial coefficient is almost as large as the second one (van der Schoot & Odijk 1992). Currently, there is a lack of both experiments and theories describing the I–N transition in suspensions of attractive rods and our understanding of the phase behaviour of rods with attraction is rather limited.

We should note that there is a recent theory that introduces attractions to the study of the I–N transition of hard rods indirectly by considering mixtures of hard rods and polymers (Lekkerkerker & Stroobants 1994). The polymers induce an effective attraction between colloidal rods through the well-known mechanism of depletion attraction (Asakura & Oosawa 1958). An advantage of this system of studying the influence of attractions on hard rods is that it is possible to control both the range of attraction by varying the molecular weight of added polymer and the interaction strength by altering the polymer concentration. However, there is an important difference between a hard-rod–polymer mixture and suspension of pure rods with attractive interactions, because for the latter the polymer concentration is different across the coexisting phases and therefore the strengths of attraction between rods in the isotropic and nematic phases are different (Lekkerkerker *et al.* 1992).

In our experimental studies of mixtures of fd wild type and polymers, we seek polymers that do not interact with the virus. The two polymers we use for this purpose are PEG and Dextran. To measure the I–N phase coexistence, we mix concentrated fd virus and Dextran (MW 148 000), dilute the sample with buffer until two-phase coexistence is initiated, and let the sample phase separate at room temperature, which takes about two weeks for the slowest phase-separating sample. The R_g of 148 000 Dextran is *ca.* 11 nm (Nordmeier 1993; Senti *et al.* 1955). In order to measure the

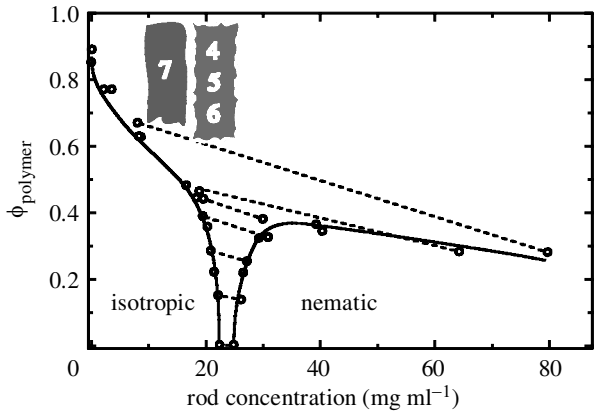

Figure 3. Phase diagram of fd wild type and Dextran (MW 148 000) mixture at 200 mM ionic strength. The R_{g} of Dextran was taken to be 11 nm and the vertical axis is given by $\phi_{\mathrm{polymer}} = \frac{4}{3}\pi R_{\mathrm{g}}^3 (N/V)$, where N/V is the number density of Dextran polymers. The dashed lines are tie-lines between coexisting isotropic and nematic (cholesteric) phases. For clarity, not all the coexistence lines are shown. The full lines are a guide to the eye, indicating the boundary of the two-phase region. At high polymer concentrations, the rods do not form a uniform phase, but a percolating network that does not completely sediment, and therefore we are not able to measure its concentration. The region of the phase diagram labelled 4–7 corresponds to the conditions of the samples in figures 4–7, although the ionic strengths are different. In this region of the phase diagram, tie-lines connect the isotropic and smectic phases.

concentration of both rods and polymers in the coexisting isotropic and nematic phases, we use fluorescently labelled FITC-Dextran. After appropriate dilution, the concentrations of both polymer and fd are measured on the spectrophotometer. The resulting phase diagram is shown in figure 3. At low polymer volume fraction, the coexisting I–N concentrations change little from the pure virus limit and there is little polymer partitioning between the coexisting phases. At higher polymer volume fractions, the phase diagram 'opens up' and we measure the coexistence between a polymer-rich rod-poor isotropic phase and a polymer-poor rod-rich nematic phase. The qualitative features in such a phase diagram are very similar to the theoretically predicted phase diagram (Lekkerkerker & Stroobants 1994; Bolhuis *et al.* 1997). In a forthcoming publication, we will present detailed experiments of the effects of ionic strength, polymer nature and molecular weight on the phase diagram.

When the phase diagram 'opens up', the concentration of rods in the nematic phase coexisting with the isotropic phase dramatically increases. For the ionic strength of 100 mM, fd virus forms a stable smectic phase at 160 mg ml^{-1} (Dogic & Fraden 1997), so it is reasonable to expect a stable isotropic–smectic (I–S) phase coexistence to supersede the I–N transition for high enough polymer volume fraction, which is, indeed, the case. Since the size of our virus allows us to visualize individual smectic layers with an optical microscope, we can observe the nucleation and growth of the smectic phase out of an isotropic suspension in real time. Observation of typical structures and their temporal evolution are summarized in the remainder of this paper. All the following images were taken with a Nikon optical microscope using DIC optics equipped with a 60× water immersion lens and condenser. Our previous work on mixtures of rods and spheres focused on the nematic–smectic phase transition, where we employed fd as rods and for spheres used either polymers, such

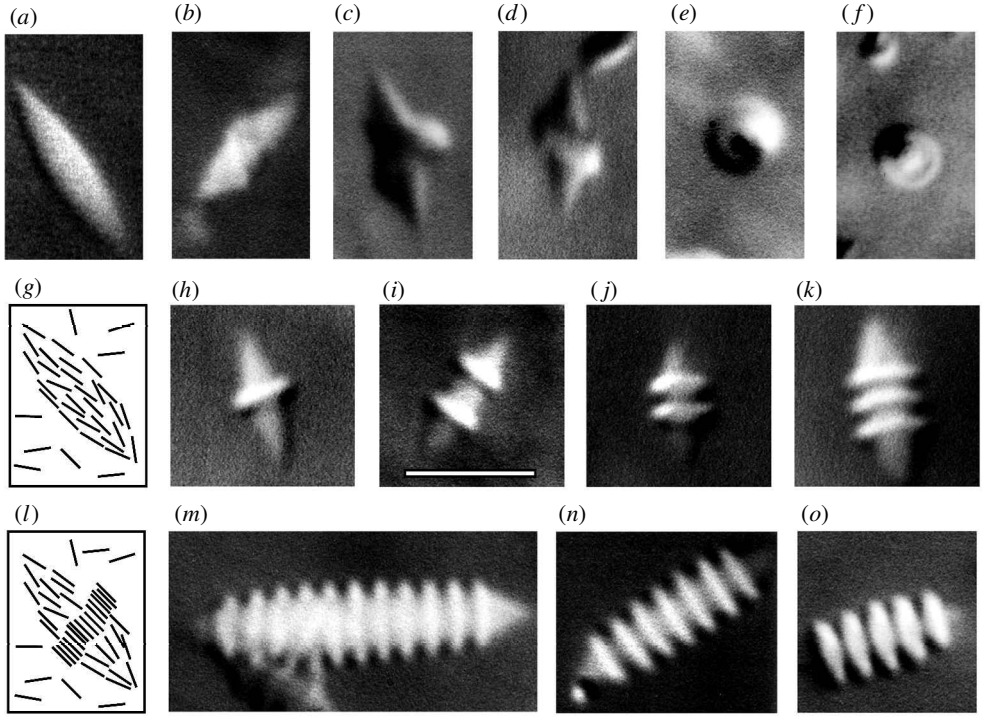

Figure 4. Initial kinetics of the isotropic–smectic phase transition of an initially isotropic suspension of fd at a concentration of 22 mg ml^{-1} and Dextran (MW 150 000), which shows the formation of striped tactoids upon addition of Dextran. The ionic strength is 110 mM. The initial step is a formation of metastable nematic drops (a), which serve as nucleation sites for the formation of single-layer smectics. The concentration of polymer in images (a)–(f) and (h)–(k) is constant and was added to the pure virus suspension until it became slightly turbid. The concentration of polymer increases in samples (m)–(o). In sample (g) we sketch the conformation of rods in a typical nematic tactoid at the I–N transition observed for rods with no, or small amounts of, attraction. The sketch of a nematic tactoid with a single smectic ring corresponding to (h) is shown in (l). The scale bar is 5 μm long and all images are taken at the same magnification.

as Dextran or PEG, or polystyrene latex with diameters ranging from 40–100 nm, distinct from the work here, which focuses on the isotropic–smectic transition using smaller polymers of diameters 4–10 nm (Adams *et al.* 1998; Dogic *et al.* 2000).

A homogeneous sample of composition in the part of the two-phase region of figure 3 where the tie-lines connect the isotropic and nematic phases begins phase separation by forming nematic ellipsoidal tactoids, as shown in figure 4*a*. The tactoids are nematic because they are too small to fit the cholesteric pitch. Only when the sample has separated into bulk phases does the nematic transform into a cholesteric (Dogic & Fraden 2000). The nematic phase appears as a bright droplet elongated along the nematic director with a dark background of isotropic rods. In the figure, the rods are parallel to the plane of the paper and tend to align parallel to the I–N boundary, as illustrated in figure 4*g*. As the polymer concentration is increased further (figure 3, regions 4–7), the tie-lines connect the isotropic and smectic phases. However, we still initially observe nematic droplets, as shown in figure 4*a*, but after a

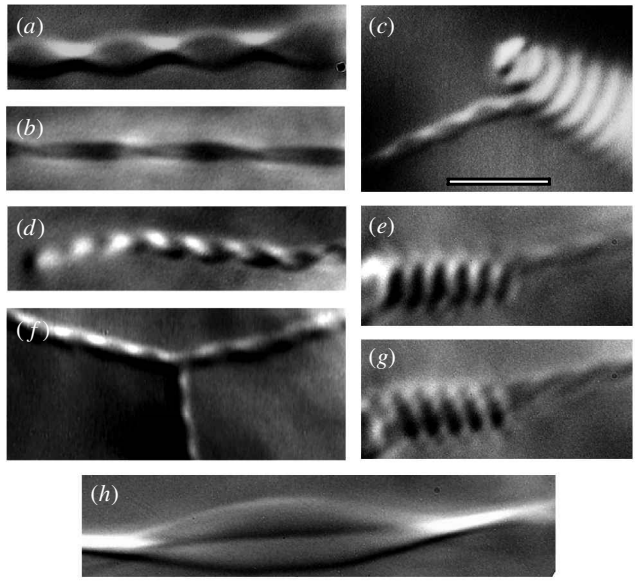

Figure 5. When the single-layer smectics form a helix on the surface of the metastable nematic drops, smectic growth continues as filaments that grow out from the nematic droplet (*c*). A helix will have layers slanted in opposite directions, as shown in (*e*) and (*g*), which show images obtained by focusing on opposite sides of the nematic nucleus. The twisted strands in (*b*)–(*g*) are with the same conditions as in figure 4*a*. Sample (*a*) is taken at a higher polymer volume fraction, while (*h*) is taken at lower virus concentrations (5 mg ml^{-1}). The scale bar indicates 5 μm.

few minutes the droplets begin to change their morphology. Parts (*a*)–(*k*) of figure 4 were all taken from the same sample and show the time-evolution of an initially smooth tactoid during the first 20–30 min of phase separation. In figure 4*b* we observe a thin helical sheet wrapped around the nematic tactoid. The width of the sheet along the direction of the tactoid is *ca.* 1 μm. We assume that this sheet is a single smectic layer of rods parallel to the direction of the nematic tactoid that has nucleated on the nematic surface. This smectic layer continues to grow and becomes thicker, as shown in the side views of the tactoid in parts (*c*) and (*d*) of figure 4. Figure 4*e* shows the same helical structure, but this time viewed from above (the alignment of the rods is perpendicular to the paper). We observe that the helical smectic layer can close upon itself to form a single toroidal ring around the nematic tactoid. A typical example of this structure is shown in figure 4*f*, where the rods are pointing out of the paper, and in figure 4*g*, where rods are parallel to the paper. Two striped tactoids with smectic rings can coalesce (figure 4*h*) to form droplets with a variable number of smectic rings, as shown in parts (*i*)–(*k*) of figure 4. Parts (*k*)–(*m*) of figure 4 are taken at increasing volume fraction of polymers. From these three parts, we observe that, with increasing polymer concentration, the thickness of the smectic rings increases in comparison with the size of the nematic core. The striped nematic droplets encircled with smectic layers will proceed to coalesce until they sediment to the bottom of the sample and reach a size that is many tens of micrometres. It should also be noted that not all tactoids have closed ring structures, but some instead have a helical

structure that has a beginning and an end. This has important consequences for the further progress of phase separation, as is demonstrated in figure 5.

After the sample has been phase separating for a few hours, we observe a new kind of structure, shown in figure 5*a*. These are filaments of fd that have a cross-section of 1 μm, which corresponds to one particle length. The director is oriented perpendicular to the fibre axis and precesses in a helical fashion, as in a cholesteric. This results in the helical structures observed in optical micrographs. The connection between the twisted sheets and the striped tactoids from figure 4 coexisting in the same sample is clearly shown in figure 5*c*. The twisted strands grow slowly out of the smectic rings and over a period of a few days the strands are able to reach lengths of several hundred micrometres. We should note that the twisted strand is a metastable structure with a pronounced tendency to untwist over a period of days or as one moves along the length of the strand away from its root at the striped I–N droplet. For example, parts (*b*)–(*g*) of figure 5 were all taken from the sample and show very different degrees of twisting. Two strands can also connect with each other, as is shown in figure 5*f*. The twisted strands can quite often form a helical superstructure. Figure 5*e* is focused on the bottom and figure 5*g* is focused on the top of such a structure. Perhaps such a structure has its origin in a striped tactoid (figure 5*c*) that has, for some reason, lost its nematic core.

After a few months, as the sample further evolves towards equilibrium, we observe a number of large sheets that are one rod length thick. We believe that these are essentially large single-layer smectic membranes. Using the microscope, we photograph a sequential series of images in the plane of focus (*xy*-plane, figure 6*a*), evenly spaced at 0.2 μm intervals in the *z*-direction, and from this information we reconstruct the structure of the membrane in three dimensions. Figure 6*c* shows the image of the membrane perpendicular to the alignment of the rods, from which we deduce that the diameter of the membrane is *ca.* 10 μm. The cuts through the *xy*- and *yz*-planes are uniformly 1 μm thick along the *y*-direction.

In another series of experiments, we studied a mixture of fd virus and PEG polymer (MW 35 000, $R_g = 9.6$ nm), shown in figure 7. The concentration of rods (10 mg ml^{-1}) was lower than in the Dextran–virus mixture described previously, but the ionic strength was again 110 mM. We increased polymer concentration until we observed slight turbidity in our sample, indicating the onset of two-phase coexistence. The structures we observed under these conditions with PEG–virus mixtures are very similar to the structures observed in Dextran–virus mixtures illustrated in the previous three figures. As we increased the polymer concentration further, we observed a direct formation of the smectic membrane out of isotropic suspension, instead of their growth from the striped nematic tactoid. An image of such a membrane, where all the rods point out of the surface of the paper, is shown in figure 7*a*. The side view (not shown) indicates that the membrane is essentially one rod-length thick. The membranes are stable over a period of hours, which is surprisingly long. If the sample is observed for long enough, it is possible to observe the process of coalescence of two smectic membranes. Figure 7*e* shows such a process in a sequence of frames spaced $\frac{1}{30}$ s apart. In the first frame, the rods in both membranes are aligned in the same direction. Once the membranes are aligned, the process of coalescence is complete in *ca.* 0.16 s.

As the concentration of the polymer is increased further, another pathway to the formation of the smectic phase is observed. We presume that this process initially

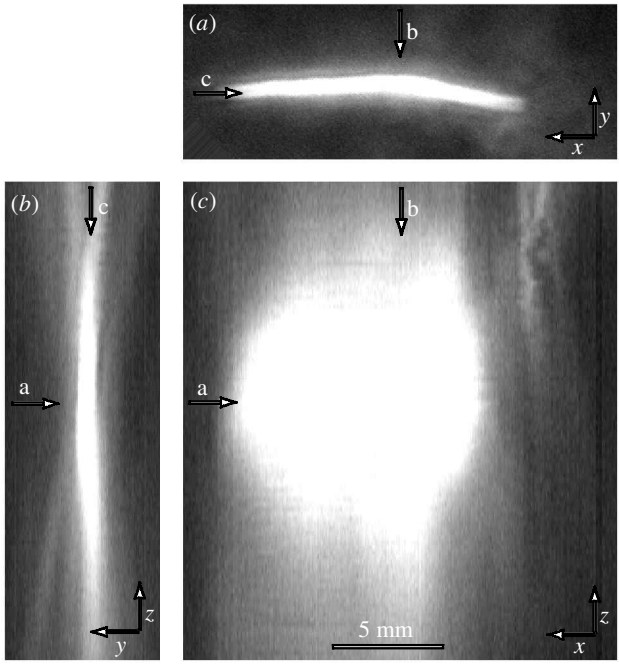

Figure 6. A three-dimensional reconstruction of a large membrane of a single-layer smectic that is observed in a mixture of fd wild type and Dextran 150 000 MW after it has been equilibrating for two months. The tubes of smectic, approximately one rod length in diameter (illustrated in figure 5), have now been transformed into extended sheets one rod length thick. Using the microscope, a sequential series of images in the xy-plane at different depths z (sample (a)) were taken and the image was reconstructed in three dimensions. (b) The image of the membrane cut along the y-direction at the position indicated by arrow b in samples (a) and (c). Equivalently, (c) shows the cut of the membrane perpendicular to the virus axis as indicated by arrow c in sample (a) and (b). The scale bar indicates 5 μm.

begins with the formation of the smectic membranes, just as the one described in the previous paragraph does. However, these membranes never reach the size of the membranes at lower polymer concentration, which coalesce sideways, as is shown in figure 7*e*. Instead, while the membranes are quite small, they stack on top of each other to form long filaments, shown in figure 7*c*. Within a few seconds of mixing the sample these filaments form a percolating network, which is self-supporting and does not sediment over time. As is seen in figure 7*c*, the thickness of the filament is not uniform, but varies from one layer to the other. The irregular thickness of the filaments does not change, even if the sample is left to equilibrate for few days. From this we can conclude that it takes rods a very long time to diffuse from one layer to another. We also observe that, as the concentration of the polymer is increased, the thickness of the filament decreases. The formation of the filaments can be understood in terms of depletion attraction. Once a single smectic layer grows to a critical size, a lower energy is achieved by stacking two equal diameter membranes on top of each other rather than by letting two membranes coalesce laterally. This is because the strength of the attraction between two surfaces is proportional to the area of the interacting surfaces.

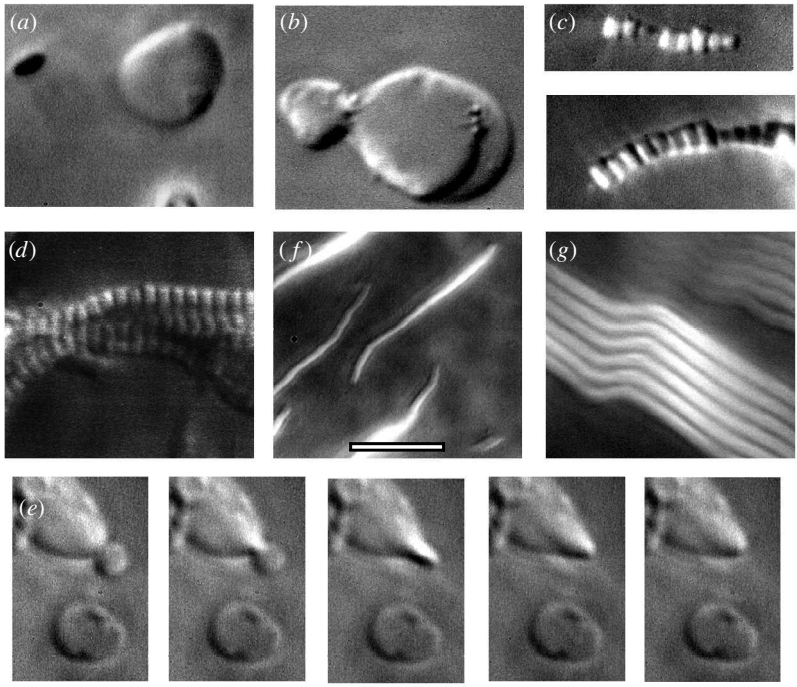

Figure 7. Phase behaviour of mixture fd and PEG (MW 35 000). At the lowest concentrations of polymer, we observe striped tactoids that are very similar to the ones shown in previous figures. As the polymer concentration is increased, we observe formation of a single membrane one rod-length thick, shown in (*a*) and (*b*). In (*e*), five successive video frames, spaced $\frac{1}{30}$ s apart, show coalescence of two smectic membranes. At an even higher volume fractions of polymer, we observe filaments (shown in (*c*) and (*d*)) that percolate throughout the entire sample. The phase transitions on the surface are shown in (*f*) and (*g*). The scale bar indicates 5 μm.

It is well known that depletion attraction between a colloid and a wall is much stronger than the attraction between two colloids (Dinsmore *et al.* 1997; Sear 1998). Because of this, in parallel to the bulk phase transitions described previously, there are competing transitions with the surface of the container. Some of the structures we observe on the surfaces due to the depletion attraction are shown in parts (*f*) and (*g*) of figure 7. Figure 7*f* shows a single smectic layer of rods. By focusing through the layer in the z-direction, we conclude that this layer is extremely thin (upper limit of 0.2 μm). Furthermore, these layers can stack on top of each other, as is shown in figure 7*g*.

Up to now, all the experiments have been done with polymers of roughly the same radius of gyration (Dextran 150 000 has $R_g = 11$ nm, PEG 35 000 has $R_g = 9.6$ nm) and at same ionic strength (110 mM). When we decrease the radius of the polymer (PEG 8000 has $R_g = 4.1$ nm), we still observe two-dimensional membranes that are composed of parallel rods. However, as is shown in figure 8, the membranes assume a hexagonal shape, which strongly implies that the rods within the membrane are not two-dimensional fluids, but two-dimensional crystals. Parts (*a*)–(*d*) of figure 8 were taken at the lowest polymer concentration at which the crystallization was observed.

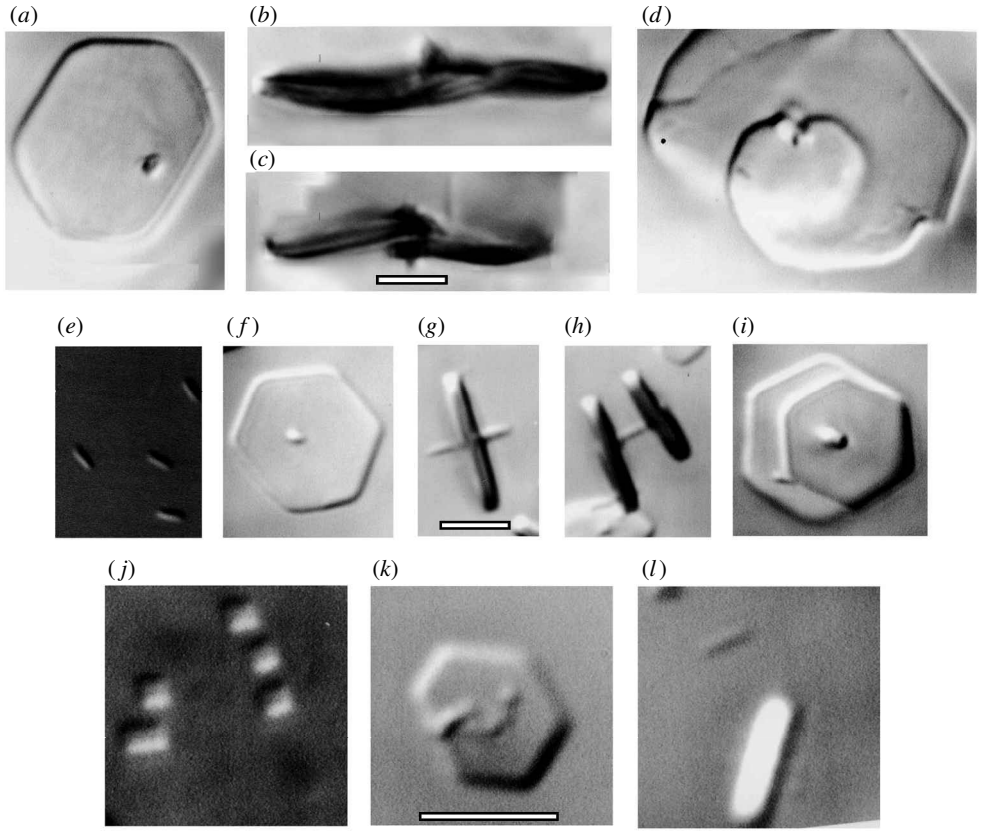

Figure 8. Optical micrographs of two-dimensional virus crystals observed in a mixture of PEG (MW 8000) and fd virus at a constant virus concentration of 15 mg ml^{-1}. The first row of images is at the lowest polymer concentration at which the crystals where observed, the second row is at an intermediate polymer concentration, and the third row is at the highest polymer concentration. All crystals are penetrated by a thin filament, which serves as the nucleation site of the crystal and forms 30 min after mixing the sample (image (*e*)). The scale bars are 5 μm, and images in each row are at the same magnification.

Under these conditions, the induction time for critical nuclei formation, as indicated by the turbidity of the sample, is *ca.* 30 min. A typical image of a two-dimensional crystal, where the rods within the crystal are pointing out of the plane of the paper, is shown in figure 8*a*, while the side view, where the alignment of the rods is in the plane of the paper, is shown in figure 8*b*. The thermal fluctuations within the crystal are easily visible under the microscope and the crystal is readily deformed, as is visible in the side view of the crystal. Often, instead of observing a flat membrane, we observe a membrane with screw dislocation located at the nucleation centre. The images of such a membrane from the top and side views are shown in parts (*c*) and (*d*) of figure 8, respectively. In figure 8*c* we can clearly see that the two layers are on top of each other, but if we focus through in the z-direction, we observe that these two layers belong to the same two-dimensional crystal. This is exactly what we would expect from a crystal that has a screw dislocation.

If we increase the polymer concentration, the induction time decreases and an

image of these post-critical nuclei is shown in figure 8*e*. A typical crystal that usually grows overnight out of this solution is shown in top view in figure 8*f*, while figure 8*g* shows the side view of such a crystal. A nucleation centre that significantly protrudes out of the two-dimensional crystalline membrane in clearly visible, and sometimes it is even possible to observe two two-dimensional crystal membranes connected through the same nucleation centre, as shown in figure 8*h*. The nucleation centres, which are long thin needles (figure 8*e*), appear in the first few minutes after making a sample. It is important to note that such a nucleation centre is visible in every two-dimensional crystalline membrane and at all polymer concentrations. Two-dimensional crystals have been observed in rod-like TMV–BSA mixtures (Adams & Fraden 1998) and these crystals also have a clearly visible single nucleation site protruding. The fact that the structures observed in PEG–fd and TMV–BSA systems are extremely similar suggest that the features of the two-dimensional crystalline membranes summarized here are generic to any system of rods with short-range attraction. Parenthetically, we note the resemblance of the virus crystals of figure 8 to 'shish-kebabs', which is the name given to lamellar crystals, grown around a central fibre, that are observed in polymer crystallization from solution and melt (Pennings *et al.* 1977). But whether or not the mechanisms governing shish-kebab and two-dimensional virus crystal formations are related is not clear.

At even higher polymer concentrations, the induction time is immeasurably short, and typical nuclei that are formed almost instantaneously are shown in figure 8*j*. The resulting crystals display almost no thermal fluctuations, are much smaller than crystals formed at low polymer concentrations, have a much higher number density, and typically their edges are much sharper and better defined, as is shown in parts (*k*) and (*l*) of figure 8.

The influence of both polymer concentration and polymer range has been extensively studied for three-dimensional spherical colloids (Hagen & Frenkel 1994; Gast *et al.* 1986; Lekkerkerker *et al.* 1992). The basic parameter that determines the behaviour of the system is the ratio of the range of attraction between colloids to the range of the effective hard core repulsion. On the one hand, if the range of attraction is very short, the vapour–liquid phase transition will be metastable with regards to the vapour–crystal transition for all conditions. On the other hand, if the range of attraction is sufficiently long ranged under certain conditions, the vapour–liquid transition will supersede the vapour–crystal phase transition. Our results on the formation of two-dimensional membranes in the polymer–virus mixtures agree with this general rule. In the mixture of large polymer (Dextran MW 150 000, $R_g = 11$ nm) and fd virus, the attraction is long ranged and we observe a two-dimensional liquid-like membrane. It contrast, in the mixture of small polymer (PEG 8000, $R_g = 4$ nm), where the attraction is short ranged, we observe a two-dimensional crystalline membrane.

5. Conclusions

In the first two sections of this paper we described the production of monodisperse rod-like fd and M13 viruses for which the contour length and effective diameter were systematically altered. We plan to use these viruses to study smectic phase formation as a function of the ratio of contour length to persistence length, and to use the polymer-grafted fd to study smectic phase formation as a function of the range of

interparticle repulsion. We also plan to study the effects of bidispersity and polydispersity, in both diameter and length, on the liquid crystalline phase transitions. In the latter portion of this paper, we summarized the kinetics of the isotropic–smectic phase transition of virus–polymer mixtures. Although the interactions between rods in polymer solutions is very simple, we observe novel structures of surprising complexity. The observed nucleation pathway is richer than envisioned previously in theory (Hohenberg & Swift 1995), or even observed in simulation (ten Wolde & Frenkel 1999). These experiments and previous studies on rod–sphere mixtures (Adams *et al*. 1998) indicate that there is much that remains to be understood about the phase behaviour of such mixtures.

This research was supported by an NSF grant. We thank Kirstin Purdy for preparation of the cloned virus pGT-N28. Additional information, movies and photographs are available online at www.elsie.brandeis.edu.

References

Adams, M. & Fraden, S. 1998 Phase behavior of mixtures of rods (tobacco mosaic virus) and spheres (polyethylene oxide, bovine serum albumin). *Biophys. J.* **74**, 669.

Adams, M., Dogic, Z., Keller, S. L. & Fraden, S. 1998 Entropically driven microphase transitions in mixtures of colloidal rods and spheres. *Nature* **393**, 349.

Asakura, S. & Oosawa, F. 1958 Interactions between particles suspended in solutions of macromolecules. *J. Polymer Sci.* **33**, 183.

Bates, M. A. & Frenkel, D. 1998 Influnce of polydispersity on the phase behavior of colloidal liquid crystals: a Monte Carlo simulation study. *J. Chem. Phys.* **109**, 6193–6199.

Bhattacharjee, S., Glucksman, M. J. & Makowski, L. 1992 Structural polymorphism correlated to surface charge in filamentous bacteriophages. *Biophys. J.* **61**, 725.

Bohle, A. M., Holyst, R. & Vilgis, T. 1996 Polydispersity and ordered phases in solutions of rodlike macromolecules. *Phys. Rev. Lett.* **76**, 1396–1399.

Bolhuis, P. G. & Frenkel, D. 1997 Tracing the phase boundaries of hard spherocylinders. *J. Chem. Phys.* **106**, 668–687.

Bolhuis, P. G., Stroobants, A., Frenkel, D. & Lekkerkerker, H. N. W. 1997 Numerical study of the phase behavior of rodlike colloids with attractive interactions. *J. Chem. Phys.* **107**, 1551.

Chen, Z. Y. 1993 Nematic ordering in semiflexible polymer chains. *Macromolecules* **26**, 3419.

Cui, S. & Chen, Z. Y. 1994 Columnar and smectic order in binary mixtures of aligned hard cylinders. *Phys. Rev.* E **50**, 3747.

Devanand, K. & Selser, J. C. 1991 Asymptotic behavior and long-range interactions in aqueous solutions of poly(ethylene oxide). *Macromolecules* **24**, 5943.

Dinsmore, A. D., Warren, P. B., Poon, W. C. K. & Yodh, A. G. 1997 Fluid–solid transitions on walls in binary hard-sphere mixtures. *Europhys. Lett.* **40**, 337–342.

Dogic, Z. & Fraden, S. 1997 Smectic phase in a colloidal suspension of semiflexible virus particles. *Phys. Rev. Lett.* **78**, 2417.

Dogic, Z. & Fraden, S. 2000 Cholesteric phase in virus suspensions. *Langmuir* **16**, 7820–7824.

Dogic, Z., Frenkel, D. & Fraden, S. 2000 Enhanced stability of layered phases in parallel hard spherocylinders due to addition of hard spheres. *Phys. Rev.* E **62**, 3925–3933.

Fraden, S. 1995 Phase transitions in colloidal suspensions of virus particles. In *Observation, prediction and simulation of phase transitions in complex fluids* (ed. M. Baus, L. F. Rull & J. P. Ryckaert), pp. 113–164. Dordrecht: Kluwer.

Gast, A. P., Russel, W. B. & Hall, C. K. 1986 An experimental and theoretical study of phase transitions in the polystyrene latex and hydroxyethylcellulose system. *J. Colloid Interface Sci.* **109**, 161.

Hagen, M. H. J. & Frenkel, D. 1994 Determination of phase diagram for the hard-core attractive Yukawa system. *J. Chem. Phys.* **101**, 4093–4097.

Herrmann, R., Neugebauer, K., Pirkl, E., Zentgraf, H. & Schaller, H. 1980 Conversion of bacteriophage fd into an efficient single-stranded DNA vector system. *Molec. Gen. Genet.* **177**, 231–242.

Hohenberg, P. C. & Swift, J. B. 1995 Metastability in fluctuation-driven first-order transitions: nucleation of lamellar phases. *Phys. Rev.* E **52**, 1828–1845.

Koda, T. & Kimura, H. 1994 Phase diagram of the nematic–smectic A transition of the binary mixture of parallel hard cylinders of different lengths. *J. Phys. Soc. Japan* **63**, 984.

Kuhl, T. L., Leckband, D. E., Lasic, D. D. & Isrealachvii, J. N. 1994 Modulation of interaction forces between bilayers exposing short-chained ethylene oxide headgroups. *Biophys. J.* **66**, 1479.

Lekkerkerker, H. N. W. & Stroobants, A. 1994 Phase behaviour of rod-like colloid + flexible polymer mixtures. *Nuovo Cim.* D **16**, 949.

Lekkerkerker, H. N. W., Coulon, P., der Haegen, V. & Deblieck, R. 1984 On the isotropic–nematic liquid crystal phase separation in a solution of rodlike particles of different lengths. *J. Chem. Phys.* **80**, 3427–3433.

Lekkerkerker, H. N. W., Poon, W. C. K., Pusey, P. N., Stroobants, A. & Warren, P. B. 1992 Phase behavior of colloid + polymer mixture. *Europhys. Lett.* **20**, 559.

Livolant, F. 1991 Ordered phases of DNA *in vivo* and *in vitro*. *Physica* A **176**, 117–137.

Maguire, J. F., McTague, J. P. & Rondalez, F. 1980 Rotational diffusion of sterically interaction rodlike macromoleculse. *Phys. Rev. Lett.* **45**, 1891–1894.

Maniatis, T., Sambrook, J. & Fritsch, E. F. 1989 *Molecular cloning*. New York: Cold Spring Harbor University Press.

Meyer, R. B. 1990 Ordered phases in colloidal suspensions of tobacco mosaic virus. In *Dynamics and patterns in complex fluids* (ed. A. Onuki & K. Kawasaki), p. 62. Springer.

Nordmeier, E. 1993 Static and dynamic light-scattering solution behavior of pullulan and dextran in comparison. *J. Phys. Chem.* **97**, 5770.

Onsager, L. 1949 The effects of shape on the interaction of colloidal particles. *Ann. NY Acad. Sci.* **51**, 627.

Pennings, A. J., Lageveen, R. & DeVries, R. S. 1977 *Coll. Polymer Sci.* **255**, 532.

Polson, J. M. & Frenkel, D. 1997 First-order nematic–smectic phase transtion for hard spherocylinders in the limit of infinite aspect ratio. *Phys. Rev.* E **56**, 6260.

Sato, T. & Teramoto, A. 1994 Statistical mechanical theory for liquid-crystalline polymer solutions. *Acta Polymer* **45**, 399–412.

Sear, R. P. 1998 Depletion driven adsorption of colloidal rods onto a hard wall. *Phys. Rev.* E **57**, 1983–1989.

Sear, R. P. & Mulder, B. M. 1996 Phase behavior of a symmetric binary mixture of hard rods. *J. Chem. Phys.* **105**, 7727–7734.

Senti, F. R., Hellman, N. N., Ludwig, N. H., Babcock, G. E., Tobin, R., Glass, C. A. & Lamberts, B. L. 1955 Viscosity, sedimentation and light-scattering properties of fractions of an acid-hydrolyzed dextran. *J. Polymer Sci.* **17**, 527.

Stroobants, A. 1992 Columnar versus smectic order in binary mixtures of hard parallel spherocylinders. *Phys. Rev. Lett.* **69**, 2388.

Stroobants, A., Lekkerkerker, H. N. W. & Odijk, T. 1986 Effect of electrostatic interaction on the liquid crystal phase transition in solutions of rodlike polyelectrolytes. *Macromolecules* **19**, 2232.

Tang, J. & Fraden, S. 1995 Isotropic–cholesteric phase transition in colloidal suspensions of filamentous bacteriophage fd. *Liq. Cryst.* **19**, 459–467.

ten Wolde, P. R. & Frenkel, D. 1999 Homogeneous nucleation and the Ostwald step rule. *Phys. Chem. Chem. Phys.* **1**, 2191–2196.

Tkachenko, A. V. 1996 Nematic–smectic transition of semiflexible chains. *Phys. Rev. Lett.* **77**, 4218–4221.

van der Schoot, P. 1996 The nematic–smectic transition in suspensions of slightly flexible hard rods. *J. Physique II* **6**, 1557.

van der Schoot, P. & Odijk, T. 1992 Statistical theory and structure factor of semidilute solution of rodlike macromolecules interacting by van der waals forces. *J. Chem. Phys.* **97**, 515–524.

van Roij, R. & Mulder, B. 1996 Demixing versus ordering in hard rod mixture. *Phys. Rev.* E **54**, 6430.

van Roij, R., Mulder, B. & Dijkstra, M. 1998 Phase behavior of binary mixture of thick and thin hard rods. *Physica* A **261**, 374–390.

Vroege, G. J. & Lekkerkerker, H. N. W. 1992 Phase transitions in lyotropic colloidal and polymer liquid crystals. *Rep. Prog. Phys.* **8**, 1241.

Wen, X., Meyer, R. B. & Caspar, D. L. D. 1989 Observation of smectic-A ordering in a solution of rigid-rod-like particles. *Phys. Rev. Lett.* **63**, 2760.

Discussion

R. Jones (*Department of Physics, Queen Mary, University of London, UK*). You have measured the order parameter in the nematic phase for a range of volume fractions. Is there any possibility that you could measure the order parameter in the smectic phase?

S. Fraden. To measure the nematic order parameter in either the nematic or smectic phase requires having a single domain sample. We achieve this by using a small lightweight permanent magnet of 2 T strength (Hummingbird Instruments, Arlington, MA, USA) to align nematic fd samples in a 0.7 mm quartz cylindrical capillary. This field strength is sufficient to align all but the most concentrated of the virus nematic samples (Dogic & Fraden 2000). Smectic samples, by contrast, will not align even when placed in 20 T fields and all our attempts to align smectics have failed, which has prevented us from measuring the angular distribution in the smectic phase. However, the smectic samples are ordered enough to measure the smectic density order parameter. Previously we have made light scattering measurements of the relative scattered intensity from smectic samples to determine the structure of the smectic phase (Dogic & Fraden 1997). It would require repeating those experiments and measuring the absolute scattering intensity to obtain the smectic density order parameter.

I. Hamley (*School of Chemistry, University of Leeds, UK*). Concerning your results showing the formation of smectic tactoids in an isotropic matrix, have you made any comparisons with the theory of Hohenberg & Swift (1995) for the nucleation of a smectic phase in a fluctuation-driven first-order transition?

S. Fraden. Dr Hamley inquires as to the relevance of the theory of Hohenberg & Swift (1995) to our observations of the kinetics of the isotropic–smectic transition. In the work of Hohenberg & Swift, the nucleating droplets are considered to be smectic, although they may be anisotropic or spherical in shape, have sharp or diffuse interfaces and contain or be free of defects. However, we never observe the scenario envisioned by Hohenberg & Swift. Instead, for low amounts of added polymer, the nucleating droplet is nematic, not smectic (see figure 4). We assume that the effective attraction between the virus rods is an increasing function of added polymer. The

observation of a metastable nematic drop is consistent with Ostwald's rule of stages, which states that phase transformation begins with the phase with free-energy closest to the starting phase, regardless of whether it is the equilibrium phase. Again, it would be reasonable to expect that the nematic droplets would transform into smectic droplets of the class considered by Hohenberg & Swift, but instead of this reasonable scenario of continued Ostwald ripening from the metastable nematic to stable smectic, a different process is observed. As described in figure 4, the smectic phase nucleates on the outside surface of metastable nematic droplets as a single-layer smectic. If the single-layer smectic forms a helix, as illustrated in figure 5, then the smectic continues to grow as a filament that gradually transforms into an extended sheet of single-layer smectic, as shown in figure 6. If the initial concentration of added polymer is higher than for figure 4, the nucleating phase is a single-layer smectic, as shown in figure 7, and, for still higher polymer concentrations, two-dimensional crystals, as opposed to smectics, are observed (figure 8).

If, following Onsager, we claim that the colloidal viruses serve as a reference hard-particle system, then we would predict that the scenario experimentally observed (in contrast to the scenario proposed by Hohenberg & Swift) would be indicative of a wide class of physical systems. We wish to mention that a member of this audience remarked that the details of the two-dimensional crystals with their nucleating filament (figure 8) are reminiscent of the 'shish-kebab' structures observed in the crystallization of polymers from solution. Whether or not the analogy arises from universal behaviour of hard-particle systems remains to be seen.

I. Hamley. Could you comment on the origin of the unwinding of cholesteric helices from tactoids that you observe?

S. Fraden. It is not clear how the winding occurs in the first place, as the smectic filaments on the nematic droplets do not appear chiral (figure 5*c*). In fact, we understand very little of this phenomenon and can only speculate that the unwinding occurs as the smectic order develops because twist is incompatible with a smectic.

I. Hamley. Given that the Onsager theory for the orientational distribution function does not account for your measured order parameters, and attractive interactions between rods are present, have you made comparisons with the Maier–Saupe theory?

S. Fraden. The order parameter at the I–N transition for the Maier–Saupe theory is $S \sim 0.5$, while we measure a higher value of $S \sim 0.65$. We still believe that the virus liquid crystals are best described as a lyotropic hard-rod system with, perhaps, some attraction that can be treated as a perturbation to the hard-particle reference system.